Cell, Vol. 110, 361–371, August 9, 2002, Copyright ©2002 by Cell Press

PGR5 Is Involved in Cyclic Electron Flow around Photosystem I and Is Essential for Photoprotection in *Arabidopsis*

Yuri Munekage,[1] Masaya Hojo,[1] Jörg Meurer,[2] Tsuyoshi Endo,[3] Masao Tasaka,[1] Toshiharu Shikanai[1,4]

[1]Graduate School of Biological Sciences
Nara Institute of Science and Technology
Ikoma, Nara 630-0101
Japan

[2]Ludwig-Maximilians-Universität
Botanisches Institut
Menzinger Strasse 67
D-80638 München
Germany

[3]Graduate School of Biostudies
Kyoto University
Sakyouku, Kyoto 606-8502
Japan

Summary

During photosynthesis, plants must control the utilization of light energy in order to avoid photoinhibition. We isolated an *Arabidopsis* mutant, *pgr5* (*proton gradient regulation*), in which downregulation of photosystem II photochemistry in response to intense light was impaired. *PGR5* encodes a novel thylakoid membrane protein that is involved in the transfer of electrons from ferredoxin to plastoquinone. This alternative electron transfer pathway, whose molecular identity has long been unclear, is known to function in vivo in cyclic electron flow around photosystem I. We propose that the PGR5 pathway contributes to the generation of a ΔpH that induces thermal dissipation when Calvin cycle activity is reduced. Under these conditions, the PGR5 pathway also functions to limit the overreduction of the acceptor side of photosystem I, thus preventing photosystem I photoinhibition.

Introduction

Light energy is converted into chemical energy by the function of two photosystems located in the chloroplast thylakoid membranes. They operate in tandem to produce a linear flow of electrons from H_2O to $NADP^+$ while accumulating reducing power in the forms of reduced ferredoxin or NADPH in the stroma. At the same time, electron transport through the cytochrome b_6f complex, an intermediate between the two photosystems, generates a proton gradient across the thylakoid membrane (ΔpH) that is utilized in ATP synthesis. These first stable products of photosynthesis are used in various metabolic reactions, including CO_2 fixation. In addition to this linear electron transport, ATP can be produced from cyclic electron flow around photosystem I (PSI), wherein electrons are recycled from reduced ferredoxin or NADPH to plastoquinone functioning in electron transport from photosystem II (PSII) to the cytochrome b_6f complex (reviewed in Bendall and Manasse, 1995).

Cyclic electron flow around PSI was first discovered based on its coupling with ATP synthesis approximately 50 years ago (cyclic phosphorylation) (Arnon et al., 1954, 1967; Arnon 1959; Arnon and Chain, 1975), prior to the discovery of linear electron flow. It is most likely that cyclic electron flow around PSI contributes to the generation of ATP in cyanobacteria (Mi et al., 1995), the green alga *Chlamydomonas reinhardtii* (Ravenel et al., 1994; Finazzi et al., 2002), and possibly in C_4 plants (Asada et al., 1993). In contrast, the recycling of electrons around PSI is rather insignificant in C_3 plants (Herbert et al., 1990; Joët et al., 2002), implying that ATP synthesis is achieved solely by linear electron flow during photosynthesis. Due to its unknown significance and perhaps the lack of definitive methods for its evaluation (Bendall and Manasse, 1995), cyclic electron flow around PSI has long been overlooked especially in C_3 plants, where the details of the process have yet to be established.

The generation of ΔpH also induces downregulation of PSII photochemistry under excessive light conditions in addition to its role in ATP synthesis. This process is called "thermal dissipation" because excessive light energy is safely dissipated as heat from PSII, therefore avoiding the production of triplet chlorophylls that react with molecular oxygen. Thermal dissipation is induced by acidification of the thylakoid lumen (ΔpH generation), which depends on the photosynthetic electron transport. This implies that the electron transport is feedback regulated via thermal dissipation. Under stress conditions, such as those produced by low temperature, drought, and nutrient depletion, the utilization of the reducing power in CO_2 fixation is limited. Limitation of electron acceptance from PSI suppresses electron transport activity. The important physiological question of how ΔpH is maintained under such conditions has not yet been answered. It is possible that alternative electron transport pathways, including cyclic electron flow around PSI, can induce thermal dissipation under these conditions, given that these pathways are independent of energy utilization (Heber and Walker, 1992; Niyogi, 1999). The idea of cyclic electron flow around PSI has been revived due to its possible function in photoprotection (Bendall and Manasse, 1995; Heber and Walker, 1992).

Interestingly, the chloroplast genome of higher plants contains eleven genes encoding homologs of a mitochondrial respiratory complex, NDH (Matsubayashi et al., 1987). Chloroplast reverse genetics has helped to assess the possibility that the chloroplastic NDH complex catalyzes the electron flow from NAD(P)H to plastoquinone and functions in cyclic electron flow around PSI (Burrows et al., 1998; Shikanai et al., 1998), as in cyanobacteria (Ogawa, 1991; Mi et al., 1995). Although chloroplastic NDH catalyzes such electron flow, the complete disruption of genes encoding the NDH complex did not affect photosynthesis, at least under greenhouse conditions (Burrows et al., 1998; Shikanai et al., 1998). However, NDH may be redundant with another

[4]Correspondence: shikanai@bs.aist-nara.ac.jp

pathway of cyclic electron flow around PSI, the antimycin A-sensitive, ferredoxin-dependent pathway (Endo et al., 1998; Joët et al., 2001). This idea is supported by evidence that cyclic electron flow around PSI was first recognized as a ferredoxin-dependent plastoquinone reduction (FQR) activity in vitro (Tagawa et al., 1963; Mills et al., 1979). Although FQR possibly catalyzes the main pathway of cyclic electron flow around PSI rather than NDH in higher plants, the molecular identity of FQR has not been revealed so far. Present understanding on cyclic electron flow around PSI has increased only marginally from the time the original concept was established, some 40 years ago.

Our concept is that the defect in the main pathway of cyclic electron flow around PSI should cause the insufficient ΔpH generation, leading to the reduced induction of thermal dissipation under excessive light conditions. Induction of thermal dissipation can be monitored by the high chlorophyll fluorescence at high light intensity (Krause and Weis, 1991), which can be utilized in the isolation of *Arabidopsis thaliana* mutants affecting the induction of thermal dissipation (Shikanai et al., 1999). Here, we describe one of the mutants, *pgr5* (*proton gradient regulation*), displaying the high chlorophyll fluorescence at high light intensity. The *PGR5* gene encodes a novel protein involved in the cyclic electron flow around PSI playing a central role in the acidification of the thylakoid lumen, thus inducing thermal dissipation. We provide evidence that PGR5 functions in the photoprotection of PSI under conditions of acceptor side limitation, by draining electrons trapped in PSI.

Results

Electron Transport Was Restricted Specifically at High Light Intensity in *pgr5*

Steady-state chlorophyll fluorescence captured by a charge-coupled device (CCD) camera was compared between the wild-type and *pgr5* at a light intensity of 300 μE/m^{2}s (Figure 1A). Light energy absorbed by light-harvesting pigments is transmitted to the PSII reaction center, where a small part of energy is emitted as chlorophyll fluorescence. The fluorescence level is indicative of the excitation state of PSII reaction center and thus lowered by the utilization of light energy (photochemical quenching). At high light intensity, excitation energy of chlorophyll molecules in antennae is dissipated as heat (thermal dissipation) and is not transmitted to the reaction center. This regulatory process induces the quenching of chlorophyll fluorescence and is the main cause of nonphotochemical quenching (NPQ) in higher plants (Krause and Weis, 1991). Although chlorophyll fluorescence was lowered in the wild-type, *pgr5* still emitted a high level of chlorophyll fluorescence under the same light conditions (Figure 1A). With respect to seedling size, *pgr5* showed normal photoautotrophic growth when growing on soil at a low light intensity (50 μE/m^{2}s).

Photosynthetic electron transport was characterized in detail by comparing the light intensity dependence of chlorophyll fluorescence parameters between *pgr5* and the wild-type using pulse-amplitude modulated (PAM) chlorophyll fluorometry (Figures 1B and 1C). PAM facilitates quantitative analysis of the fluorescence signal, which is utilized in the calculation of each parameter (see Experimental Procedures for details). The relative electron transport rate (ETR) through PSII was not affected in *pgr5* at low light intensities below 100 μE/m^{2}s (Figure 1B) and is consistent with the normal growth rate at 50 μE/m^{2}s. However, the ETR was near saturation point at 300 μE/m^{2}s in the wild-type and was saturated at 100 μE/m^{2}s at the lower level (60% of the maximum ETR in the wild-type) in *pgr5* (Figure 1B).

NPQ was induced with an increase in light intensity in the wild-type; however, this induction was significantly reduced in *pgr5* (Figure 1C). NPQ is caused mainly by the thermal dissipation of excitation energy from PSII, which is triggered by lumenal acidification. This ΔpH-

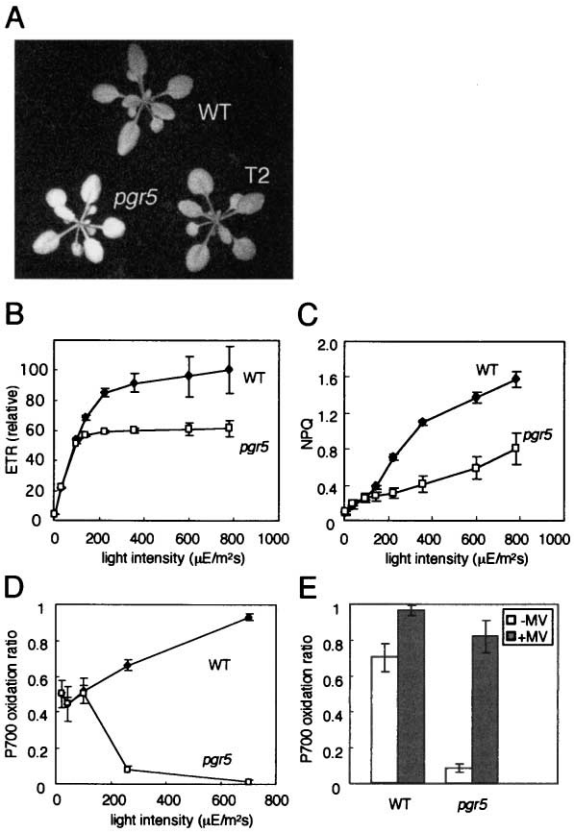

Figure 1. Characterization of *pgr5*

(A) High chlorophyll fluorescence phenotype of *pgr5*. Dark-adapted seedling of the wild-type (wt), *pgr5*, and *pgr5* transformed with the wild-type genomic *PGR5* sequence (T2) were illuminated at 300 μE/m^{2}s for 1 min, and then a chlorophyll fluorescence image was captured by a CCD camera.

(B) Light intensity dependence of the relative electron transport rate (ETR) in *pgr5* and the wild-type leaves. ETR was represented as relative values of the maximum ETR in the wild-type (100%). Means $\pm$ SD (n = 3).

(C) Light intensity dependence of nonphotochemical quenching (NPQ) of chlorophyll fluorescence in *pgr5* and the wild-type leaves. Means $\pm$ SD (n = 3).

(D) Light intensity dependence of the P700 oxidation ratio ($\Delta A/\Delta Amax$) in *pgr5* and the wild-type leaves. Means $\pm$ SD (n = 3).

(E) P700 oxidation ratio at a light intensity of 800 μE/m^{2}s in the presence (+MV) or the absence (−MV) of methyl viologen. Methyl viologen (2 μM) was infiltrated into leaf disks prior to the analysis. Means $\pm$ SD (n = 3).

dependent NPQ is characterized by its rapid relaxation kinetics, occurring within 3 min in the dark. Although a small amount of NPQ (0.8) was induced in *pgr5* at 800 $\mu E/m^2s$, it failed to relax within 3 min in the dark (data not shown), indicating that the NPQ formed in *pgr5* did not depend on ΔpH. The remaining NPQ in *pgr5* may possibly be due to photoinhibition and/or the movement of peripheral light-harvesting antennae from PSII to PSI (state transition). Thermal dissipation is induced by the acidification of the thylakoid lumen, which is caused by the transport of electrons through the cytochrome b_6f complex. The induction of thermal dissipation is impaired, most likely by the restricted electron transport rate at high light intensity. This situation was evident in the cytochrome b_6f mutant, *pgr1,* characterized by Munekage et al. (2001).

Electron Acceptance from PSI Was Conditionally Impaired in *pgr5*

To specify the *pgr5* defect in photosynthetic electron transport, it is informative to monitor the electron flow through PSI during steady-state photosynthesis, as well as that through PSII monitored by chlorophyll fluorescence (Figures 1B and 1C). Figure 1D shows the redox state of the PSI reaction center (P700) in the light. P700 is reduced in the dark, but is oxidized to $P700^+$ by PSI photochemistry in the light. Oxidation can be monitored by absorbance changes at 830 nm (Schreiber et al., 1988). We examined the light intensity dependence of the P700 oxidation ratio ($\Delta A/\Delta Amax$) in the wild-type and *pgr5* (Figure 1D). The maximum level of $P700^+$ ($\Delta Amax$) was determined by far-red light illumination, which preferentially activates PSI photochemistry. In the wild-type, P700 was oxidized at a close to linear rate with increasing light intensity. This is due to the down-regulation of PSII photochemistry (thermal dissipation) and the restriction of electron transport at the cytochrome b_6f complex. The P700 redox state was indistinguishable between *pgr5* and the wild-type at light intensities below 100 $\mu E/m^2s$; however, it was dramatically lowered with increasing light intensities in *pgr5* (Figure 1D).

The low P700 oxidation ratio in *pgr5* may be caused by the reduction of $P700^+$ by electrons that have returned from a series of acceptor side electron carriers in PSI (A_0, A_1, F_X, and F_A/F_B). This phenomenon is referred to as a charge recombination of P700 and is caused by the overreduction of electron acceptors from PSI, ferredoxin, and $NADP^+$ (Endo et al., 1999). A charge recombination of P700 can also be caused by a nonfunctional acceptor chain in PSI (Golbeck and Bryant, 1991). In the former case, the $P700^+$ level can be restored by the addition of methyl viologen (MV), which is an artificial electron acceptor from PSI. We used MV at a low concentration (2 μM) to avoid the possibility of direct electron acceptance from P700 (Sonoike and Terashima, 1994). In the presence of MV, the P700 oxidation ratio in *pgr5* was similar to that in the wild-type at a light intensity of 800 $\mu E/m^2s$ (Figure 1E). The chlorophyll fluorescence parameters, ETR and NPQ, were also restored by adding MV (data not shown). These results indicate that limited electron acceptance from PSI caused a charge recombination of P700 in *pgr5* rather than a nonfunctional acceptor chain in PSI.

Table 1. Quantum Yield of PSII (Φ_{PSII}) in the Ruptured Chloroplasts

	Φ_{PSII}	
Genotype (Acceptors)	50 $\mu E/m^2s$	200 $\mu E/m^2s$
Wild-type (MV)	0.52 ± 0.03	0.21 ± 0.03
pgr5 (MV)	0.50 ± 0.04	0.19 ± 0.01
Wild-type (Fd+$NADP^+$)	0.48 ± 0.02	0.17 ± 0.01
pgr5 (Fd+$NADP^+$)	0.49 ± 0.02	0.20 ± 0.02

To confirm that PSI activity in *pgr5* is unaffected, linear electron transport to $NADP^+$ was measured in ruptured chloroplasts with exogenous electron acceptors (Table 1). The electron transport rate was estimated as the quantum yield of PSII (Φ_{PSII}), which is calculated from chlorophyll fluorescence parameters (Genty et al., 1989). When MV was added as an artificial electron acceptor, the Φ_{PSII} was identical in *pgr5* and the wild-type at light intensities of 50 $\mu E/m^2s$ and 200 $\mu E/m^2s$. Ferredoxin and $NADP^+$ were also added to mimic in vivo electron transport conditions. The Φ_{PSII} remained unchanged in *pgr5* at both light intensities. We conclude that the PSI activity, including electron donation to ferredoxin and subsequent $NADP^+$ reduction, is not affected in *pgr5*.

PGR5 Encodes a Novel Protein Associated with Thylakoid Membranes

The *pgr5* mutation was mapped to the north region of chromosome II, between the molecular markers RNS1 and SNP184 (Figure 2A). Genomic sequences of genes containing predicted plastid-targeting signals (predicted by Predotar; http://www.inra.fr/Internet/Produits/Predotar/) from *pgr5* and the wild-type were compared. A nucleotide substitution was found in the second exon of the gene (At2g05620/T20G20.3 in Figure 2A). The mutation led to an amino acid substitution from glycine to serine. At2g05620 encodes a protein consisting of 133 amino acids with a predicted molecular mass of 14 kDa. Highly homologous proteins were found in other photosynthetic organisms, including soybean, rice, volvox, *Chlamydomonas*, and *Synechocystis* PCC6803 (Figure 2B), but not in nonphotosynthetic organisms such as *Escherichia coli* and yeast. The program ChloroP 1.1 (http://www.cbs.dtu.dk/services/ChloroP/) predicted the cleavage site of the transit peptide to be after the 44th amino acid.

To confirm that the *pgr5* phenotype was due to the mutation in At2g05620, *pgr5* was transformed with the wild-type genomic sequence of At2g05620. The normal chlorophyll fluorescence level was restored in the transformant lines (T2 in Figure 1A). Restoration of the normal electron transport activity was also confirmed by analysis of PAM chlorophyll fluorometry and the P700 oxidation ratio in the light (data not shown).

To characterize the gene product PGR5, antibodies were raised against a synthetic oligopeptide of PGR5. Western analysis revealed a 10 kDa protein, which was absent in *pgr5* (Figure 2C, lanes 1 and 2). In complemented *pgr5* mutant lines, the 10 kDa protein was present (Figure 2C, lane 3), confirming that the signal corresponded to PGR5. The 10 kDa peptide is consistent with the predicted mature form of PGR5 (9.8 kDa) minus

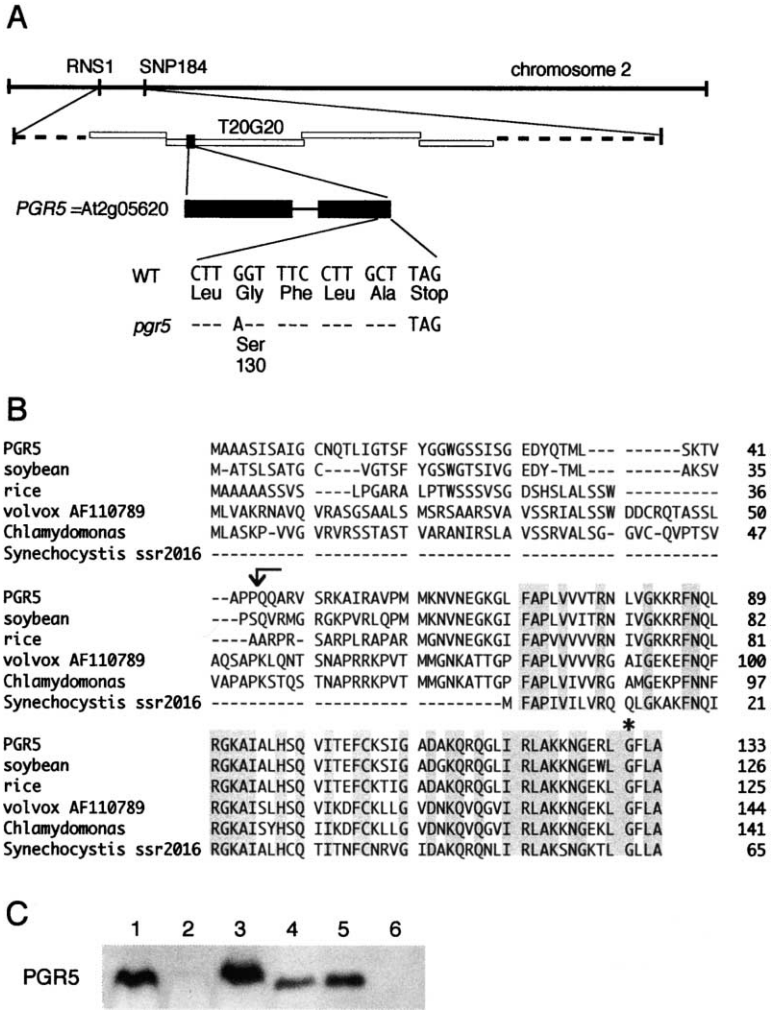

Figure 2. Map-Based Cloning of *pgr5*

(A) *pgr5* was mapped between the molecular makers RNS1 and SNP184 on chromosome 2 using 340 F_2 plants. Open boxes represent bacterial artificial chromosome clones. *PGR5* was the gene At2g05620 (T20G20.3). A single nucleotide substitution was found in the second exon of At2g05620, leading to an amino acid substitution from glycine 130 to serine. Closed boxes represent exons.

(B) Alignment of the amino acid sequences of PGR5 homologs. Shaded sequences are conserved among PGR5, the PGR5 homologs from soybean, rice, *Chlamydomonas*, and volvox, and *Synechocystis* PCC6803. The asterisk indicates the *pgr5* mutation site. An arrow indicates the predicted cleavage site of the transit peptide.

(C) Western analysis of PGR5. Total proteins from the wild-type (lane 1), *pgr5* (lane 2), and *pgr5* transformed with the wild-type sequence (lane 3) were applied. Total chloroplast proteins were extracted from the wild-type (lane 4) and then fractionated into the thylakoid membrane (lane 5) and the stroma (lane 6). Sample loading was standardized by chlorophyll content (2.0 μg).

its transit sequence (Figure 2B). Although the *pgr5* mutation leads to a minor amino acid substitution from glycine to serine, the mutated form of PGR5 is unstable in vivo (Figure 2C, lane 2).

Chloroplasts purified from wild-type leaves were subjected to Western analysis. When the sample load was standardized for chlorophyll content, an equal signal intensity of PGR5 was detected for total leaf proteins and chloroplast proteins (Figure 2C, lanes 1 and 4). The result confirms that PGR5 is present in chloroplasts. To determine the PGR5 localization in chloroplasts, chloroplast preparations were further fractionated into soluble proteins (stroma fraction) and thylakoid membranes. The PGR5 signal was detected in the thylakoid membrane but not in the stroma fraction (Figure 2C, lanes 5 and 6). From this result we conclude that PGR5 is a thylakoid membrane protein. Computer-aided analysis failed to reveal a transmembrane region in PGR5, suggesting that PGR5 associates with the thylakoid membranes peripherally or via interaction with other thylakoid membrane proteins.

PGR5 Functions in Alternative Electron Transport from PSI

In *pgr5*, electron acceptance from PSI was impaired specifically at high light intensity. However, the electron transport activity to $NADP^+$ via ferredoxin was not affected (Table 1). The normal photoautotrophic growth rate in *pgr5* (Figure 1A) suggests that PGR5 is not involved in the main pathway of photosynthetic electron flow to CO_2. PGR5 may function in alternative electron transport pathways, which become important when electron acceptance by $NADP^+$ is limited. To assess this possibility, alternative electron flow capacity was estimated based on the level of $P700^+$ under artificial air conditions (Figure 3). In CO_2-free air, inhibition of CO_2 assimilation leads to depletion of $NADP^+$, which stimulates alternative electron transport activity. We also measured the $P700^+$ level in N_2 gas (CO_2- and O_2-free air), where O_2-dependent alternative pathways, including photorespiration and electron transport to O_2 (water-water cycle), were inhibited. Photorespiration involves an unnecessary consumption of NADPH and ATP due to the oxygenase activity of ribulose 1,5-bisphosphate carboxylase/oxygenase under certain conditions. Such activity causes a relaxation in the overreduction of the stroma (Kozaki and Takeba, 1996). The water-water cycle is triggered by the photo-reduction of O_2 to superoxide, which can also act as an alternative electron acceptor from PSI (reviewed in Asada, 1999). Since both O_2-dependent pathways are inhibited in N_2 gas, we have

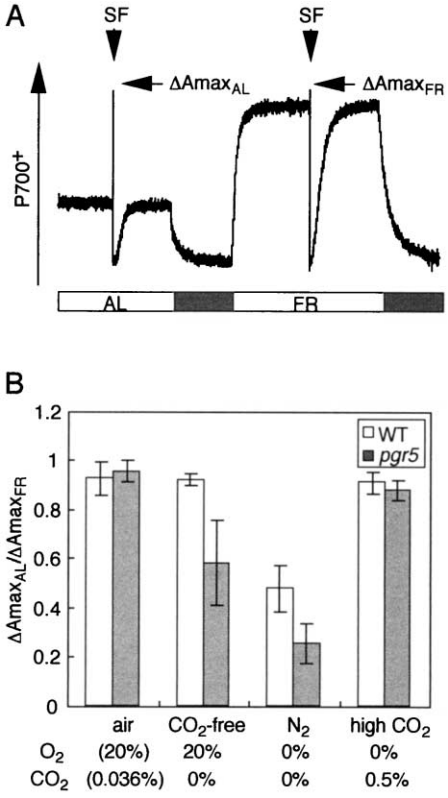

Figure 3. Analysis of Alternative Electron Flow Activity

(A) Strategy to determine the capacity of alternative electron flow. The limitation of electron acceptors from PSI was evaluated by reduction in the $P700^+$ level. Representative absorbance changes at 830 nm are shown in a wild-type leaf in the air. Xenon flashes of saturating light (SF) were applied to monitor ΔAmax during the illumination period of actinic light ($\Delta Amax_{AL}$) and far-red light (Δmax_{FR}). A white bar under graphs indicates the periods of illumination with actinic light (AL, >650 nm, 50 μE/m^{2}s) or far-red light (FR, 720 nm, 0.66 μE/m^2 s), and a black bar indicates darkness.

(B) Limitation of electron acceptance from PSI was evaluated from $\Delta Amax_{AL}/\Delta Amax_{FR}$ in the wild-type and *pgr5* in the air, CO_2-free air, N_2 gas, and high-CO_2 air (0.5% CO_2 and O_2-free air). Means ± SD (n = 6).

been able to estimate the capacity of O_2-independent pathways, including cyclic electron flow around PSI.

The strategy for determining the capacity of alternative electron flow estimated from the $P700^+$ level is represented by the pattern that the wild-type produces in the air (Figure 3A). A saturating xenon flash of 50 ms (SF) will instantly oxidize P700 to a high level by PSI photochemistry. This is followed by the rapid reduction by electrons from PSII, and subsequently the steady-state oxidation level is gradually restored. The top of the peak generated by SF represents the maximum $P700^+$ level during actinic light (AL) illumination ($\Delta Amax_{AL}$). When electron acceptors from PSI (oxidized ferredoxin or O_2) are limited during actinic light illumination, the maximum $P700^+$ level decreases due to electrons returning from acceptor side electron carriers in PSI (A_0, A_1, F_X, and F_A/F_B). In contrast, a xenon flash under the weak, far-red light (FR) background will cause the full oxidation of P700 ($\Delta Amax_{FR}$) (Endo et al., 1999). Thus, the limitation in electron acceptors from PSI can be evaluated as a decrease in $\Delta Amax_{AL}/\Delta Amax_{FR}$. In this assay, we used a low actinic light intensity (50 μE/m^{2}s) at which electrons are predominately used for CO_2 fixation in the air.

In air, $\Delta Amax_{AL}/\Delta Amax_{FR}$ was approximately 1 in both the wild-type and *pgr5*, indicating that electron acceptors from PSI were not limited in both plants (Figure 3B). In CO_2-free air, acceptor limitation was not observed in the wild-type ($\Delta Amax_{AL}/\Delta Amax_{FR} = 1$), indicating electrons were drained via an alternative electron transport from PSI. However, in *pgr5*, the $\Delta Amax_{AL}/\Delta Amax_{FR}$ was lowered to 0.6, indicating electrons were trapped for a longer period of time in PSI due to the reduced activity of the alternative electron transport. In N_2 gas, acceptor limitation was observed even in the wild-type ($\Delta Amax_{AL}/\Delta Amax_{FR} = 0.5$), indicating that O_2-dependent pathways function as significant electron acceptors from PSI in CO_2-free air. If the *pgr5* is defective in O_2-dependent alternative electron transport pathways, the levels of $\Delta Amax_{AL}/\Delta Amax_{FR}$ in N_2 gas should be identical between *pgr5* and the wild-type. However, electron acceptors were more severely limited in *pgr5* ($\Delta Amax_{AL}/\Delta Amax_{FR} = 0.3$) than in the wild-type.

To confirm that PGR5 functions in the alternative electron flow from PSI, O_2-free air was supplemented with a high concentration (0.5%) of CO_2. Under these conditions, electrons were preferentially used for CO_2 fixation, and electron acceptance from PSI was almost completely restored in both the wild-type and *pgr5* ($\Delta Amax_{AL}/\Delta Amax_{FR} = 0.9$). These results indicate that *pgr5* is defective in at least the O_2-independent alternative pathway. The contribution of the PGR5-related alternative pathway(s) is physiologically significant in draining electrons from PSI under acceptor-limiting conditions, such as in CO_2-free air.

Cyclic Electron Transport around PSI Was Impaired in *pgr5*

The most likely alternative pathway involving PGR5 is the cyclic electron flow around PSI, which mediates the electron transport from ferredoxin to plastoquinone (Figure 4A). To assess this possibility, the cyclic electron transport activity of donating electrons to plastoquinone from ferredoxin was assayed with ruptured chloroplasts in the dark. Plastoquinone reduction was monitored as an increase in chlorophyll fluorescence emitted by the exposure of light with a very low intensity (1.0 μE/m^{2}s). At this light intensity, the fluorescence level predominately reflects the reduction of plastoquinone by cyclic electron transport from ferredoxin, not by PSII photochemistry. While the addition of NADPH induced only a slight increase of chlorophyll fluorescence in the wild-type, the addition of ferredoxin induced a significant increase with relatively fast kinetics (t = 22 s; t is the time required to reach the maximum reduction level) (Figure 4B). In this assay system, NADPH is essential for electron donation to ferredoxin via the reverse reaction of ferredoxin-$NADP^+$ reductase (FNR) (Miyake and Asada, 1994). In contrast, the increase in chlorophyll fluorescence was slower in *pgr5* (t = 38 s) and was achieved at a much lower level. These results indicate that ferredoxin-plastoquinone reductase activity was impaired in *pgr5*.

There is physiological evidence that antimycin A inhib-

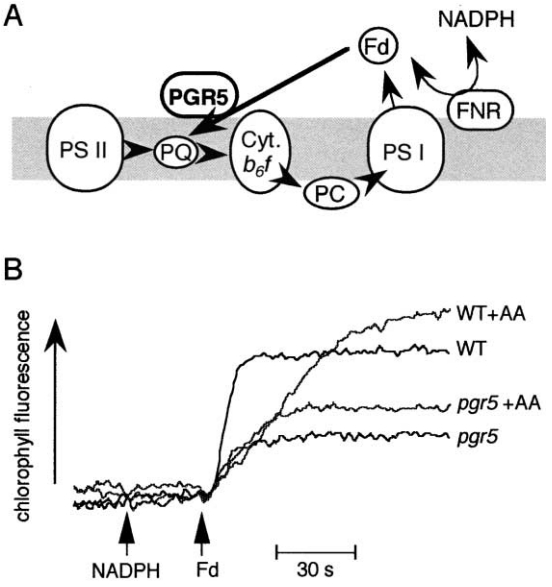

Figure 4. Electron Donation to Plastoquinone in Ruptured Chloroplasts

(A) Schematic model of electron flow from NADPH to plastoquinone (PQ) via ferredoxin (Fd) in this assay. Abbreviations: Cyt. b_6f, cytochrome b_6f complex; PC, plastocyanin.

(B) Increases of chlorophyll fluorescence by addition of NADPH (0.25 mM) and ferredoxin (Fd, 5 μM) under the illumination of weak measuring light (1.0 μE/m²s) were monitored in osmotically ruptured chloroplasts (20 μg chlorophyll/ml) of the wild-type (wt) and *pgr5*. Ruptured chloroplasts were incubated with 10 μM antimycin A (WT + AA and *pgr5* + AA) before the measurement.

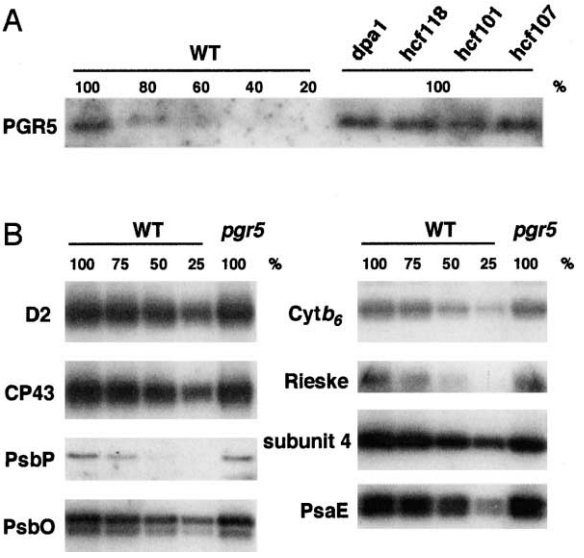

Figure 5. Reciprocal Western Analysis of Protein Stability in Mutants

(A) Immunodetection of PGR5 in photosynthetic mutants, *dpa1* lacking plastid F_1F_0 ATPase, *hcf118* lacking the cytochrome b_6f complex, *hcf101* lacking PSI, and *hcf107* lacking PSII (Meurer et al., 1996). The lanes were loaded with 10 μg protein (100%), and a series of reductions as indicated.

(B) Accumulation of PSII subunits (D2, CP43, PsbO, and PsbP), the cytochrome b_6f complex subunit (Cyt b_6, Rieske, and subunit 4), or a PSI subunit (PsaE) in *pgr5*.

its cyclic electron transport activity (Arnon et al., 1967; Mills et al., 1979). To assess the possibility that antimycin A could mimic the *pgr5* phenotype, we analyzed the effects of antimycin A in our assay system. The kinetics of plastoquinone reduction were impaired by adding antimycin A. The increase in chlorophyll fluorescence was delayed significantly in a wild-type background ($t = 79$ s), mimicking the delay seen in *pgr5*, although the final reduction level was higher (Figure 4B). In *pgr5*, the kinetics of plastoquinone reduction were not affected further by adding antimycin A ($t = 38$ s). These results indicate that PGR5 functions in a cyclic electron flow around PSI, which is inhibited by antimycin A.

PGR5 Can Stably Accumulate in Mutants of Major Complexes of Photosynthetic Electron Transport

PGR5 is a novel thylakoid protein (Figure 2), and its destabilization affects the activity of cyclic electron transport around PSI (Figure 4). It is possible that PGR5 is an accessory subunit of major complexes of the photosynthetic electron transport, which functions preferentially in cyclic electron transport around PSI. To assess this possibility, PGR5 levels were analyzed in several mutants lacking the major thylakoid membrane complexes, F_1F_0 ATPase (*dpa1*), the cytochrome b_6f complex (*hcf118*), PSI (*hcf101*), and PSII (*hcf107*) (Meurer et al., 1996; Felder et al., 2001). Figure 5A shows that PGR5 accumulated at levels comparable to those of the wild-type. We conclude that PGR5 can accumulate independently of the major complexes of the photosynthetic electron transport.

We also performed reciprocal Western analysis to evaluate the stability of the major photosynthetic complexes in *pgr5* (Figure 5B). Accumulation of PSII subunits (D2, CP43, PsbO, and PsbP), those of the cytochrome b_6f complex (Cyt b_6, Rieske, and subunit 4), or a PSI subunit (PsaE) were not affected in *pgr5*. This is consistent with the results indicating that linear electron flow was not affected in *pgr5* (Table 1). Together with the immunological data (Figure 5A), the results described above led us to conclude that PGR5 can stably accumulate independently of PSI, PSII, the cytochrome b_6f complex, and F_1F_0 ATPase and that the destabilization of PGR5 does not affect the accumulation of these complexes.

The PGR5 Pathway Functions to Induce NPQ when Electron Acceptors from PSI Are Limited

Cyclic electron flow around PSI is thought to downregulate PSII activity by acidifying the thylakoid lumen. To demonstrate the function of the PGR5 pathway in the induction of NPQ, we monitored NPQ induction during the dark-to-light (80 μE/m²s) transition. Figure 6A shows NPQ induction patterns in the air for the wild-type, *pgr5,* and the mutant *npq4-1*, which cannot induce thermal dissipation due to the lack of PsbS, an essential, specific subunit for thermal dissipation (Li et al., 2000). In the wild-type, NPQ (0.8) was transiently induced within 1 min and relaxed to 0.2 within 2 min postinduction (Figure 6A). In contrast, *npq4-1* lacked this rapid and transient

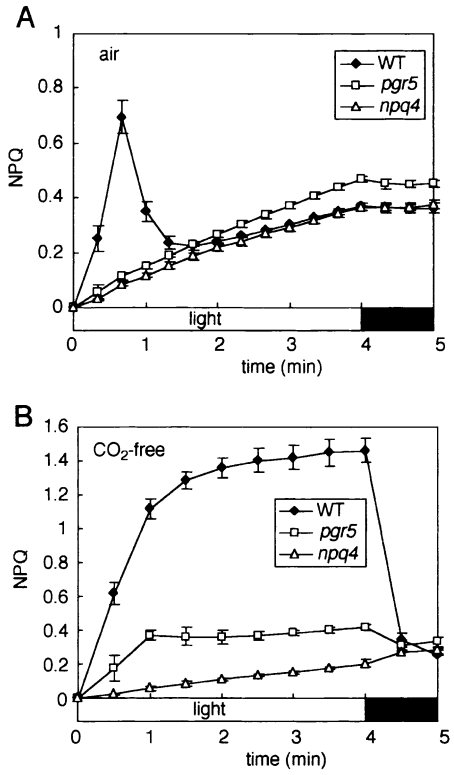

Figure 6. Time Courses of Induction and Relaxation of NPQ

Induction and relaxation of NPQ were monitored for 4 min at 80 μE/m²s illumination (a white bar) and for 1 min in the dark (a black bar), respectively, in the wild-type (wt), *pgr5,* and *npq4-1*. Analysis was performed in the air (A) or in CO_2-free air (B). Means ± SD (n = 3).

induction of NPQ, indicating that NPQ is related to thermal dissipation. Thermal dissipation is induced by the acidification of the thylakoid lumen, which occurs as a consequence of balance between the generation and relaxation of ΔpH. Thus, thermal dissipation is observed during the induction period of photosynthesis, when the relaxation of lumenal acidification by ATPase activity is not fully induced. NPQ was rapidly relaxed in the light, because 80 μE/m²s was insufficient to induce thermal dissipation during steady-state photosynthesis. Interestingly, *pgr5* completely lacked this transient increase in NPQ (Figure 6A), indicating that the thylakoid lumen was not acidified enough to induce thermal dissipation.

Figure 6B shows NPQ induction in CO_2-free air in the wild-type, *pgr5*, and *npq4-1*. In the wild-type, NPQ was induced up to 1, and was not relaxed during actinic light illumination in CO_2-free air because the relaxation of lumenal acidification was suppressed by reduced CO_2-fixation activity. Due to the defect in PsbS, *npq4-1* could not induce thermal dissipation under such conditions. A marginally higher NPQ (0.4) was induced in *pgr5* than in *npq4-1*. A part of the remaining NPQ in *pgr5* was relaxed in the dark within 1 min. Although *pgr5* can induce a small amount of thermal dissipation, the level was much lower than that induced in the wild-type. This result suggests that *pgr5* cannot acidify the thylakoid lumen when the CO_2-fixation activity is reduced. Under

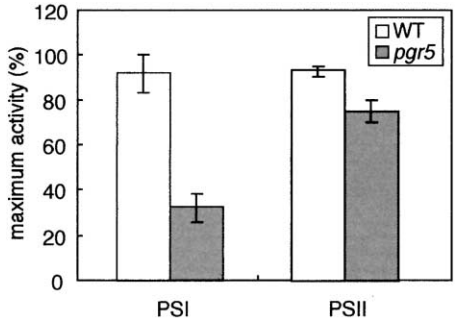

Figure 7. High Light Sensitivity of Both Photosystems

Plants grown at 50 μE/m²s were exposed to high light intensity (1500 μE/m²s) for 10 min. The photoinhibition of PSII and PSI was calculated from the maximum activities of both photosystems, Fv/Fm (PSII) and ΔAmax (PSI). Bars represent the maximum activity of photosystems after high light stress as relative values of the maximum activity in the wild-type before the stress (100%). Means ± SD (n = 5).

conditions in which the availability of $NADP^+$ is limited, such as during the dark-to-light transition and in CO_2-free air, thermal dissipation was induced by lumenal acidification generated by the PGR5-dependent alternative electron flow.

PSI Is Hypersensitive to High Light Illumination in *pgr5*

One of the typical features of *pgr5* was the reduced state of P700 at a high light intensity (Figure 1D). It has been suggested that reduction of P700 in light can lead to photodamage of PSI under stress conditions such as low temperature (Sonoike, 1996). To assess the high-light sensitivity of PSI in *pgr5*, plants grown at 50 μE/m²s were exposed to a high light intensity (1500 μE/m²s) for 10 min (Figure 7). To monitor the PSI damage, the maximum level of $P700^+$ was measured by a xenon flash under a far-red light background, before and after high light illumination. The decrease in the $P700^+$ level after high light illumination is caused not only by photoinhibition of PSI but also by an overreduced stromal state (Endo et al., 1999) and the activated cyclic electron flow (Cornic et al., 2000). To evaluate the extent of PSI photoinhibition, MV was infiltrated into the apoplast of leaves after the high-light treatment. Electron acceptance from PSI by MV restored the maximum oxidation of P700. In the wild-type, less than 10% of PSI was damaged, whereas in *pgr5*, up to 60% of PSI was damaged. We also determined the extent of PSII photodamage by measuring the maximum PSII activity (a chlorophyll fluorescence parameter, Fv/Fm). PSII photodamage was only slightly greater in *pgr5* than in the wild-type. These results indicate PSI photodamage occurs prior to PSII photodamage in *pgr5*. We conclude that the PGR5 pathway is essential for the photoprotection of PSI.

Discussion

PGR5 Functions in Cyclic Electron Flow around PSI

Our results indicate that electron transport from ferredoxin to plastoquinone is impaired in *pgr5* (Figure 4).

This electron transport pathway may function in cyclic electron flow around PSI in vivo. Although the discovery of cyclic electron flow around PSI occurred approximately 50 years ago (Arnon et al., 1954, 1967; Arnon, 1959; Tagawa et al., 1963), molecular information concerning this enigmatic pathway is still limited. However, it is known that the chloroplastic NDH complex, which is considered to have originated from a cyanobacterial respiratory complex, functions in cyclic electron flow around PSI in higher plants (Burrows et al., 1998; Shikanai et al., 1998).

The following three reasons support the idea that PGR5 is not involved in NDH activity. (1) The transient increase of chlorophyll fluorescence measured immediately after turning off an actinic light, attributable to the chloroplastic NDH activity (Burrows et al., 1998; Shikanai et al., 1998; Kofer et al., 1998), is not impaired in *pgr5* (data not shown). (2) Plastoquinone reduction by ferredoxin is not affected in the absence of antimycin A in the tobacco *ndhB* knockout line (Figure 4; Endo et al., 1998). (3) The effects of *pgr5* mutations on electron transport are different from those observed in the tobacco NDH knockout lines (Figure 1; Burrows et al., 1998; Shikanai et al., 1998; Horváth et al., 2000). Therefore, we suggest that PGR5 functions in an alternative pathway of cyclic electron flow around PSI that may be redundant with NDH. Considering the obvious phenotype of *pgr5* in electron transport, we propose that the PGR5-dependent pathway is the main route of the cyclic electron flow around PSI, while the NDH-mediated pathway may play a compensatory function (Peltier and Cournac, 2002).

Ferredoxin-dependent plastoquinone reduction activity has been observed in earlier studies and was shown to be sensitive to antimycin A (Mills et al., 1979). Data are accumulating that suggest an inhibitory effect of antymicin A on cyclic electron transport activity in vivo (Tagawa et al., 1963; Heber et al., 1978; Mills et al., 1978; Moss and Bendall, 1984). We also found that antimycin A impaired plastoquinone reduction by ferredoxin in wild-type thylakoids (Figure 4). By evaluating the kinetics of plastoquinone reduction, we found that antimycin A mimicked the *pgr5* phenotype. However, the final level of plastoquinone reduction was higher in antimycin A-treated wild-type plants than in *pgr5*. A possible explanation is that antimycin A only partially inhibits the plastoquinone reduction activity. However, the double concentration of antimycin A (20 μM) did not change the result (data not shown). Clarification of the entire PGR5-dependent pathway, including the identification of the antimycin A target site(s), will help to bridge the gap between our findings and current knowledge on the subject.

PGR5 is a small protein that lacks a metal binding motif (Figure 2). Therefore, it is unlikely that PGR5 mediates the electron transport from ferredoxin to plastoquinone as an electron carrier. We speculate that the lack of PGR5 may destabilize or inactivate the complex catalyzing ferredoxin-dependent plastoquinone reduction. However, accumulation of the major complexes functioning in photosynthetic electron transport was not affected in *pgr5* (Figure 5B). Recently, the association of ferredoxin-$NADP^+$ reductase (FNR) with the cytochrome b_6f complex was reported in higher plants (Zhang et al., 2001). It is possible that the PGR5-related complex functions to donate electrons to this FNR, consequently reducing cytochrome b_6.

In addition to the PGR5-dependent cyclic electron pathway, the water-water cycle may also function as an electron acceptor from PSI (Makino et al., 2002). We concluded that the O_2-independent pathway was severely affected in *pgr5*, because the phenotype is still evident in N_2 gas, where O_2 reduction is negligible (Figure 3). Direct determination of the ferredoxin-dependent plastoquinone reduction activity also confirmed our conclusion (Figure 4). However, we still cannot rule out the possibility that the activity of O_2-dependent alternative electron flow is also affected in *pgr5*. It remains a matter of discussion as to what donates electrons to O_2 (Asada, 1999). Therefore, it is possible that O_2 reduction is mediated by the PGR5-dependent pathway and that the *pgr5* mutation may lead to pleiotropic effects on both cyclic electron transport around PSI and the water-water cycle.

PGR5 Is Essential to Induce Thermal Dissipation

Thermal dissipation plays a crucial role in the response of plants to rapid changes in light intensity (reviewed in Horton et al., 1996; Niyogi, 1999). The energy dissipation is precisely controlled by thylakoid lumenal acidification so that it would not affect the photosynthetic activity under light-limiting conditions (Munekage et al., 2001). Since the acidification of lumen depends on electron transport, this regulation functions in a feedback manner. When the consumption of reducing power in CO_2 assimilation is limited, electron transport may be slowed down by the acceptor limitation from PSI. Therefore, the compensatory mechanism should be indispensable for maintaining a ΔpH that induces thermal dissipation. In agreement with this prediction, we provide evidence that the PGR5-dependent electron transport pathway is extremely important in the induction of thermal dissipation.

Suppression of CO_2-fixation activity leads to an accumulation of excess reducing power even at a low light intensity. We propose that the PGR5-dependent electron flow generates an increased ΔpH that induces thermal dissipation under these conditions (Figure 6B). It was somewhat unexpected that ETR was mostly unaffected in CO_2-free air at a low light intensity in *pgr5* (data not shown), considering that NPQ induction was severely impaired. This result suggests that electrons must route through the PGR5 pathway to induce thermal dissipation by recycling electrons from ferredoxin to the cytochrome b_6f complex, even when other alternative pathway, probably the water-water cycle, can still accept electrons from PSI.

In comparison to CO_2-free air conditions, it is difficult to ascertain the contribution of the PGR5-pathway in induction of thermal dissipation at high light intensities in air, because linear electron transport is also affected (Figure 1B). Because the PGR5 pathway recycles electrons to the linear pathway, it is difficult to understand how the *pgr5* defect affects the efficiency of PSII photochemistry. This discrepancy can be explained by the idea that the PGR5 pathway contributes to the generation of ATP required for CO_2 fixation at high light intensi-

ties. ATP depression in *pgr5* may cause the over-reduction of the stroma, leading to reduced linear electron transport. It is thus possible that cyclic electron flow around PSI is essential for ATP synthesis during photosynthesis, as it is in photoprotection.

PGR5 Is Essential for the Photoprotection of PSI

It is generally accepted that PSII is a primary target of photoinhibition (Aro et al., 1993) and that PSI is damaged under limited conditions such as low temperature and low light illumination (Sonoike, 1996). It was surprising that PSI was damaged during high light illumination (1500 $\mu E/m^2s$ for 10 min) prior to PSII photodamage even at room temperature in *pgr5* (Figure 7). In low temperature-sensitive plants such as cucumber, the molecular mechanism of PSI photodamage is well understood (Sonoike, 1996). At low temperature, limitation of electron acceptors from PSI, which is induced by reduced CO_2-fixation activity, causes electrons to be trapped by electron carriers in the acceptor side of PSI (F_X and F_A/F_B). The reduced form of these electron carriers reacts with superoxide, resulting in the production of hydroxyl radicals, which damage PSI. *pgr5* exhibited charge recombination of P700 at high light intensities and in CO_2-free air even at low light intensities, indicating that the metal centers in the acceptor side of PSI are overreduced. We postulate that PSI is damaged in *pgr5* in a similar process with that occurring in low temperature-sensitive plants. This fact highlights the critical function of PGR5 in the photoprotection of PSI.

Experimental Procedures

Plant Materials and Growth Conditions

Arabidopsis thaliana wild-type (ecotype Columbia *gl1*) and *pgr5* were grown on soil under growth chamber conditions (50 $\mu E/m^2s$, 16 hr light:8 hr dark cycles at 23°C) for 4–5 weeks. *pgr5* was previously referred to as CE11-1-1 (Shikanai et al., 1999).

Analysis of Chlorophyll Fluorescence

An image of chlorophyll fluorescence was captured by a CCD camera after 1 min illumination of AL (300 $\mu E/m^2s$), as described previously (Shikanai et al., 1999). Chlorophyll fluorescence parameters were measured using a MINI-PAM portable chlorophyll fluorometer (Walz, Effeltrich, Germany). The minimum chlorophyll fluorescence at the open PSII center (Fo) was determined by measuring light (655 nm) at a light intensity of 0.05–0.15 $\mu E/m^2s$. A saturating pulse of white light (800 ms) was applied to determine the maximum chlorophyll fluorescence at closed PSII centers in the dark (Fm) and during AL illumination (Fm′). The steady state of the chlorophyll fluorescence level (Fs) was recorded during AL illumination (20–800 $\mu E/m^2s$). The ϕ_{PSII} at the maximum level and during steady-state photosynthesis were calculated by equations (Fm − Fo) / Fm and (Fm′ − Fs) / Fm′, respectively. The relative rate of electron transport (ETR) through PSII was calculated as $\phi_{PSII} \times$ light intensity ($\mu E/m^2s$). NPQ was calculated as (Fm − Fm′) / Fm′.

Measurement of the Absorbance Change of P700

The redox change of P700 assessed by monitoring absorbance at 830 nm was measured with a PAM chlorophyll fluorometer (Walz, Effeltrich, Germany) equipped with an emitter-detector unit ED 800T as previously described (Schreiber et al., 1988). $P700^+$ (ΔA) was recorded during red light illumination (>650 nm). The maximum contents of $P700^+$ ($\Delta Amax$) were determined using a xenon discharge lamp (50 ms, 1500 Wm^{-2}) under a far-red light background (720 nm, 0.66 $\mu E/m^2s$).

Isolation of Chloroplasts

Leaves of 4- to 5-week-old plants were homogenized in a medium containing 330 mM sorbitol, 20 mM Tricine/NaOH (pH 7.6), 5 mM EGTA, 5 mM EDTA, 10 mM $NaCO_3$, 0.1% (w/v) BSA, and 330 mg/l ascorbate. After centrifugation for 5 min at 2000 × g, the pellet was resuspended in 300 mM sorbitol, 20 mM HEPES/KOH (pH 7.6), 5 mM $MgCl_2$, and 2.5 mM EDTA. Intact chloroplasts were purified by passing through 40% Percoll.

In Vitro Assay of Linear Electron Transport Activity

Intact chloroplasts (10 μg chlorophyll/ml) were osmotically ruptured in a medium containing 50 mM HEPES/NaOH (pH 7.6), 7 mM $MgCl_2$, 1 mM $MnCl_2$, 2 mM EDTA, 30 mM KCl, and 0.25 mM KH_2PO_4. Linear electron transport activity was measured in AL with electron acceptors, 25 μM MV or 5 μM ferredoxin purified from maize, and 1 mM $NADP^+$.

In Vitro Assay of Ferredoxin-Dependent Plastoquinone Reduction Activity

Ferredoxin-dependent plastoquinone reduction activity was measured in ruptured chloroplasts as previously described (Endo et al., 1998). As electron donors, 5 μM maize ferredoxin and 0.25 mM NADPH were used.

Map-Based Cloning

The *pgr5* mutation was mapped using molecular markers based on a cleaved amplified polymorphic sequence (Konieczny and Ausubel, 1993) and simple sequence length polymorphism (Bell and Ecker, 1994). Genomic DNA was isolated from F_2 plants derived from the cross between *pgr5* (genetic background of Columbia *gl1*) and the wild-type (Landsberg *erecta*). Homozygous F_2 plants (*pgr5/pgr5*) exhibiting the high chlorophyll fluorescence phenotype were selected as described previously (Shikanai et al., 1999). At2g05620 was amplified by PCR using Ex Taq DNA polymerase (Takara, Kyoto, Japan) from the genomic DNA of the wild-type and *pgr5*. The PCR products were directly sequenced using a dye terminator cycle sequencing kit and an ABI prism377 sequencer (Perkin-Elmer, Norwalk, CT).

For complementation of the *pgr5* mutation, the wild-type genomic sequence including At2g05620 was amplified from the BAC clone T20G20 (from ATCTTGTGATCATGTGGTGC to CCAAGCGCATTA GAAGAAGA). The PCR product was subcloned into pBI101. The resulting plasmid was introduced into the *Agrobacterium tumefaciens* pMP40 strain and then into homozygous *pgr5* plants.

Immunoblot Analysis

Total cellular protein (8 μg) was fractionated through 15% SDS-PAGE and transferred to nitrocellulose membrane. Immunodetection with antibodies against an individual subunit of PSII, PSI, and the cytochrome b_6f complex was performed as described in Meurer et al. (1996). PGR5 was detected using rabbit antibodies prepared against a peptide antigen, ADAKQRQGLIRLAKKNGERL, conjugated with keyhole limpet hemocyanin.

Acknowledgments

We thank Momoko Miyata for her excellent technical assistance. We also thank Bob B. Buchanan for his critical reading of the manuscript. We are grateful to Chikahiro Miyake and Akiho Yokota for their valuable advice. Krishna K. Niyogi is gratefully acknowledged for his gift of *npq4-1* seeds. We also thank the *Arabidopsis* Biological Resource Center for the BAC clone. This work was supported by the Japan Society for the Promotion of Science (JSPS-RFTF96R16001, JSPS-RFTF00L01604, and 11640648 to T.S.) and by DFG to J.M.

Received: April 5, 2002
Revised: July 22, 2002

References

Arnon, D.I. (1959). Conversion of light into chemical energy in photosynthesis. Nature *184*, 10–21.

Arnon, D.I., and Chain, R.K. (1975). Regulation of ferredoxin-cata-

lyzed photosynthetic phosphorylations. Proc. Natl. Acad. Sci. USA *72*, 4961–4965.

Arnon, D.I., Allen, M.B., and Whatley, F.R. (1954). Photosynthesis by isolated chloroplasts. Nature *174*, 394–396.

Arnon, D.I., Tsujimoto, H.Y., and McSwain, B.D. (1967). Ferredoxin and photosynthetic phosphorylation. Nature *214*, 562–566.

Aro, E.M., Virgin, I., and Andersson, B. (1993). Photoinhibition of photosystem II. Inactivation, protein damage and turnover. Biochim. Biophys. Acta *1143*, 113–134.

Asada, K. (1999). The water-water cycle in chloroplasts: scavenging of active oxygens and dissipation of excess photons. Annu. Rev. Plant Physiol. Plant Mol. Biol. *50*, 601–639.

Asada, K., Heber, U., and Schreiber, U. (1993). Electron flow to the intersystem chain stromal components cyclic electron flow in maize chloroplasts, as detected in intact leaves by monitoring redox change of P700 and chlorophyll fluorescence. Plant Cell Physiol. *34*, 39–50.

Bell, C.J., and Ecker, J.R. (1994). Assignment of 30 microsatellite loci to the linkage map of *Arabidopsis*. Genomics *19*, 137–144.

Bendall, D.S., and Manasse, R.S. (1995). Cyclic photophosphorylation and electron transport. Biochim. Biophys. Acta *1229*, 23–38.

Burrows, P.A., Sazanov, L.A., Svab, Z., Maliga, P., and Nixon, P.J. (1998). Identification of a functional respiratory complex in chloroplasts through analysis of tobacco mutants containing disrupted plastid *ndh* genes. EMBO J. *17*, 868–876.

Cornic, G., Bukhov, N.G., Wiese, C., Bligny, R., and Heber, U. (2000). Flexible coupling between light-dependent electron and vectorial proton transport in illuminated leaves of C_3 plants. Role of photosystem I-dependent proton pumping. Planta *210*, 468–477.

Endo, T., Shikanai, T., Sato, F., and Asada, K. (1998). NAD(P)H dehydrogenase-dependent, antimycin A-sensitive electron donation to plastoquinone in tobacco chloroplasts. Plant Cell Physiol. *39*, 1226–1231.

Endo, T., Shikanai, T., Takabayashi, A., Asada, K., and Sato, F. (1999). The role of chloroplastic NAD(P)H dehydrogenase in photoprotection. FEBS Lett. *457*, 5–8.

Felder, S., Meierhoff, K., Sane, A.P., Meurer, J., Driemel, C., Plucken, H., Klaff, P., Stein, B., Bechtold, N., and Westhoff, P. (2001). The nucleus-encoded *HCF107* gene of *Arabidopsis* provides a link between intercistronic RNA processing and the accumulation of translation-competent *psbH* transcripts in chloroplasts. Plant Cell *13*, 2127–2141.

Finazzi, G., Rappaport, F., Furia, A., Fleischmann, M., Rochaix, J.-D., Zito, F., and Forti, G. (2002). Involvement of state transitions in the switch between linear and cyclic electron flow in *Chlamydomonas reinhardtii*. EMBO Rep. *3*, 280–285.

Genty, B., Briantais, J.-M., and Baker, N.R. (1989). The relationship between quantum yield of photosynthetic electron transport and quenching of chlorophyll fluorescence. Biochim. Biophys. Acta *990*, 87–92.

Golbeck, J.H., and Bryant, D.A. (1991). Photosystem I. In Current Topics in Bioenergetics: Light Driven Reactions in Bioenergetics, C.P. Lee, ed. (New York: Academic Press), pp. 83–177.

Heber, U., and Walker, D. (1992). Concerning a dual function of coupled cyclic electron transport in leaves. Plant Physiol. *100*, 1621–1626.

Heber, U., Egneus, H., Hank, U., Jensen, M., and Köster, S. (1978). Regulation of photosynthetic electron transport and photophosphorylation in intact chloroplasts and leaves of *Spinacia oleracea* L. Planta *143*, 41–49.

Herbert, S.K., Fork, D.C., and Malkin, S. (1990). Photoacoustic measurements *in vivo* of energy storage by cyclic electron flow in algae and higher plants. Plant Physiol. *94*, 926–934.

Horton, P., Ruban, A.V., and Walters, R.G. (1996). Regulation of light harvesting in green plants. Annu. Rev. Plant Physiol. Plant Mol. Biol. *47*, 655–684.

Horváth, E.M., Peter, S.O., Joët, T., Rumeau, D., Cournac, L., Horváth, G.V., Kavanagh, T.A., Schäfer, C., Peltier, G., and Medgyesy, P. (2000). Targeted inactivation of the plastid *ndhB* gene in tobacco results in an enhanced sensitivity of photosynthesis to moderate stomatal closure. Plant Physiol. *123*, 1337–1350.

Joët, T., Cournac, L., Horváth, E.M., Medgyesy, P., and Peltier, G. (2001). Increased sensitivity of photosynthesis to antimycin A induced by inactivation of the chloroplast *ndhB* gene. Evidence for a participation of the NADH-dehydrogenase complex to cyclic electron flow around photosystem I. Plant Physiol. *125*, 1919–1929.

Joët, T., Cournac, L., Peltier, G., and Havaux, M. (2002). Cyclic electron flow around photosystem I in C_3 plants. In vivo control by the redox state of chloroplasts and involvement of the NADH-dehydrogenase complex. Plant Physiol. *125*, 1919–1929.

Kofer, W., Koop, H.-U., Wanner, G., and Steinmüller, K. (1998). Mutagenesis of the genes encoding subunits A, C, H, I, J and K of the plastid NAD(P)H-plastoquinone-oxidoreductase in tobacco by polyethylene glycol-mediated plastome transformation. Mol. Gen. Genet. *258*, 166–173.

Konieczny, A., and Ausubel, F.M. (1993). A procedure for mapping *Arabidopsis* mutations using co-dominant ecotype-specific PCR-base markers. Plant J. *4*, 403–410.

Kozaki, A., and Takeba, G. (1996). Photorespiration protects C_3 plants from photoinhibition. Nature *384*, 557–560.

Krause, G.H., and Weis, E. (1991). Chlorophyll fluorescence and photosynthesis: the basics. Annu. Rev. Plant Physiol. Plant Mol. Biol. *42*, 313–349.

Li, X.-P., Björkman, O., Shih, C., Grossman, A.R., Rosenquist, M., Jansson, S., and Niyogi, K.K. (2000). A pigment-binding protein essential for regulation of photosynthetic light harvesting. Nature *403*, 391–395.

Makino, A., Miyake, C., and Yokota, A. (2002). Physiological function of the water-water cycle (Mehler reaction) and cyclic electron flow around PSI in rice leaves. Plant Cell Physiol., in press.

Matsubayashi, T., Wakasugi, T., Shinozaki, K., Yamaguchi-Shinozaki, K., Zaita, N., Hidaka, T., Meng, B.Y., Ohto, C., Tanaka, M., Kato, A., et al. (1987). Six chloroplast genes (*ndhA-F*) homologous to human mitochondrial genes encoding components of the respiratory chain NADH dehydrogenase are actively expressed: determination of the splice sites in *ndhA* and *ndhB* pre-mRNAs. Mol. Gen. Genet. *210*, 385–393.

Meurer, J., Meierhoff, K., and Westhoff, P. (1996). Isolation of high-chlorophyll-fluorescence mutants of *Arabidopsis thaliana* and their characterisation by spectroscopy, immunoblotting and Northern hybridisation. Planta *198*, 385–396.

Mi, H., Endo, T., Ogawa, T., and Asada, K. (1995). Thylakoid membrane-bound pyridine nucleotide dehydrogenase complex mediates cyclic electron transport in the cyanobacteria *Synechocystis* PCC 6803. Plant Cell Physiol. *36*, 661–668.

Mills, J.D., Slovacek, R.E., and Hind, G. (1978). Cyclic electron transport in isolated intact chloroplasts. Further studies with antimycin. Biochim. Biophys. Acta *504*, 298–309.

Mills, J.D., Crowther, D., Slovacek, R.E., Hind, G., and McCarty, R.E. (1979). Electron transport pathway in spinach chloroplasts. Reduction of the primary acceptor of photosystem II by reduced nicotinamide adenine dinucleotide phosphate in the dark. Biochim. Biophys. Acta *547*, 127–137.

Miyake, C., and Asada, K. (1994). Ferredoxin-dependent photoreduction of the monodehydroascorbate radical in spinach thylakoids. Plant Cell Physiol. *35*, 539–549.

Moss, D.A., and Bendall, D.S. (1984). Cyclic electron transport in chloroplast. The Q-cycle and the site of action of antimycin. Biochim. Biophys. Acta *767*, 389–395.

Munekage, Y., Takeda, S., Endo, T., Jahns, P., Hashimoto, T., and Shikanai, T. (2001). Cytochrome b_6f mutation specifically affects thermal dissipation of absorbed light energy in *Arabidopsis*. Plant J. *28*, 351–359.

Niyogi, K.K. (1999). Photoprotection revisited: genetic and molecular approaches. Annu. Rev. Plant Physiol. Plant Mol. Biol. *50*, 333–359.

Ogawa, T. (1991). A gene homologous to the subunit-2 gene of NADH dehydrogenase is essential to inorganic carbon transport of *Synechocystis* PCC6803. Proc. Natl. Acad. Sci. USA *88*, 4275–4279.

Peltier, G., and Cournac, L. (2002). Chlororespiration. Annu. Rev. Plant Biol. *53*, 523–550.

Ravenel, J., Peltier, G., and Havaux, M. (1994). The cyclic electron pathways around photosystem I in *Chlamydomonas reinhardtii* as determined *in vivo* by photoacoustic measurements of energy storage. Planta *193*, 251–259.

Schreiber, U., Klughammer, C., and Neubauer, C. (1988). Measuring P700 absorbance changes around 830 nm with a new type of pulse modulation system. Z. Naturforsch. *43C*, 686–698.

Shikanai, T., Endo, T., Hashimoto, T., Yamada, Y., Asada, K., and Yokota, A. (1998). Directed disruption of the tobacco *ndhB* gene impairs cyclic electron flow around photosystem I. Proc. Natl. Acad. Sci. USA *95*, 9705–9709.

Shikanai, T., Munekage, Y., Shimizu, K., Endo, T., and Hashimoto, T. (1999). Identification and characterization of *Arabidopsis* mutants with reduced quenching of chlorophyll fluorescence. Plant Cell Physiol. *40*, 1134–1142.

Sonoike, K. (1996). Photoinhibition of photosystem I: its physiological significance in the chilling sensitivity of plants. Plant Cell Physiol. *37*, 239–247.

Sonoike, K., and Terashima, I. (1994). Mechanism of photosystem I photoinhibition in leaves in leaves of *Cucumis sativus* L. Planta *194*, 287–293.

Tagawa, K., Tsujimoto, H.Y., and Arnon, D.I. (1963). Role of chloroplast ferredoxin in the energy conversion process of photosynthesis. Proc. Natl. Acad. Sci. USA *49*, 567–572.

Zhang, H., Whitelegge, J.P., and Cramer, W.A. (2001). Ferredoxin:$NADP^+$ oxidoreductase is a subunit of the chloroplast cytochrome b_6f complex. J. Biol. Chem. *276*, 38159–38165.